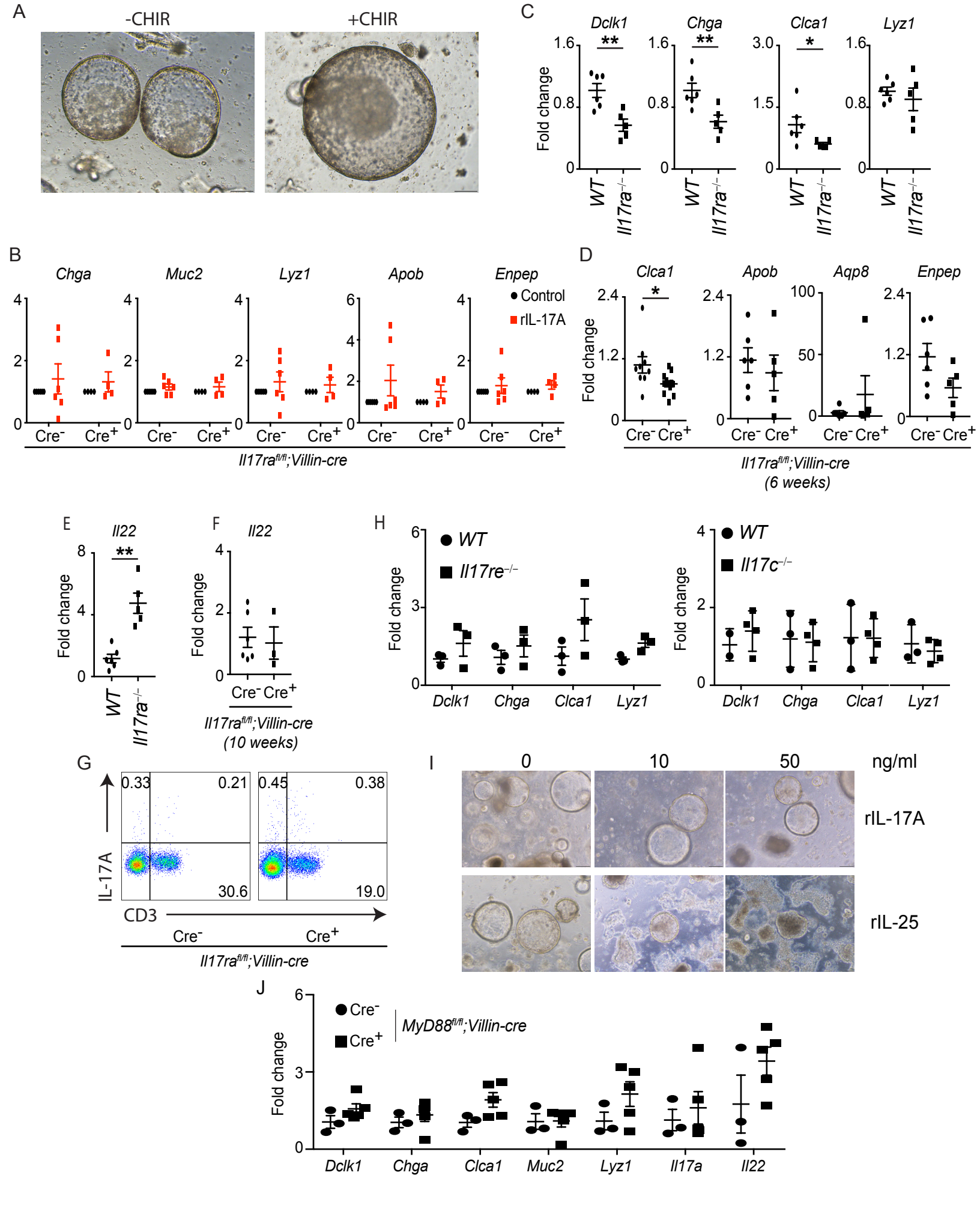
A
-CHIR
+CHIR
C
Dclk1
Chga
Clca1
Lyz1
Fold change
WT
Il17ra−/−
B
Chga
Muc2
Lyz1
Apob
Enpep
Control
rIL-17A
Cre-
Cre+
Il17rafl/fl;Villin-cre
D
Clca1
Apob
Aqp8
Enpep
Il17rafl/fl;Villin-cre
(6 weeks)
E
Il22
F
Il22
Il17rafl/fl;Villin-cre
(10 weeks)
H
WT
Il17re−/−
Il17c−/−
G
0.33
0.21
0.45
0.38
30.6
19.0
IL-17A
CD3
I
0
10
50
ng/ml
rIL-17A
rIL-25
J
MyD88fl/fl;Villin-cre
Il17a
Il22
Muc2

Supplemental Figure 1. Secretory cell defects in germ-line *Il17ra*$^{-/-}$ mice, related to Figure 1. **A)** Crypts were isolated from *Il17ra*$^{fl/fl}$*;Villin-cre* mice and seeded for organoid culture with or without CHIR99021 (CHIR). The size of organoids was monitored and the images were taken on day 6 (left panel: without CHIR; right panel: with CHIR). **B)** Crypts were isolated from *Il17ra*$^{fl/fl}$*;Villin-cre* mice for organoid culture (without CHIR99021) under the treatment of recombinant IL-17A (50 ng/ml). RNA was extracted on day 6 and the expression of *Chga, Muc2, Lyz1, Apob* and *Enpep* expression was analyzed by RT-PCR. **C)** RNA was extracted from the terminal ileum of naïve C57BL/6J (WT) and *Il17ra*$^{-/-}$ mice. The expression of *Dclk1*, *Chga, Clca1* and *Lyz1* was analyzed by RT-PCR. **D)** RNA was extracted from the terminal ileum of naïve *Il17ra*$^{fl/fl}$*;Villin-cre* mice at 6 weeks old. The expression of *Clca1, Apob, Aqp8* and *Enpep* was analyzed by RT-PCR. **E)** RNA was extracted from the terminal ileum of naïve C57BL/6J (WT) and *Il17ra*$^{-/-}$ mice. The expression of *Il22* was analyzed by RT-PCR. **F)** RNA was extracted from the terminal ileum of naïve *Il17ra*$^{fl/fl}$*;Villin-cre* mice at 10 weeks old. The expression of *Il22* was analyzed by RT-PCR. **G)** Leukocytes were isolated from the small intestine lamina propria of *Il17ra*$^{fl/fl}$*;Villin-cre* mice. Flow cytometry was utilized to analyze IL-17A production in CD45^{+} cells. **H)** RNA was extracted from the terminal ileum of *Il17re*$^{-/-}$ and *Il17c*$^{-/-}$ mice. The expression of *Dclk1, Chga, Clca1* and *Lyz1* was analyzed by RT-PCR. **I)** Crypts were isolated from the ileum of *ATOH1-EGFP* mice. Primary organoids were cultured in the presence of recombinant IL-17A or IL-25 and imaged on day 6. **J)** RNA was extracted from the terminal ileum of *MyD88*$^{fl/fl}$*;Villin-cre* mice. The expression of *Dclk1, Chga, Clca1, Muc2, Lyz1, Il17a* and *Il22* was analyzed by RT-PCR.

Figure S1B, S1D and S1F were generated from 2-3 independent experiments. Figure S1H and S1J were generated from at least 3 mice in each group. Figure S1A, S1G and S1I are the representative images of at least 3 mice in each group. Data are presented as mean± SEM in all graphs. Scale bars in relevant figures equal 100 μm (1A, 1I). *$P \leq 0.05$; **$P \leq 0.01$ (Two-Way ANOVA in B, Mann-Whitney test, two-tailed in C-F, H and J)

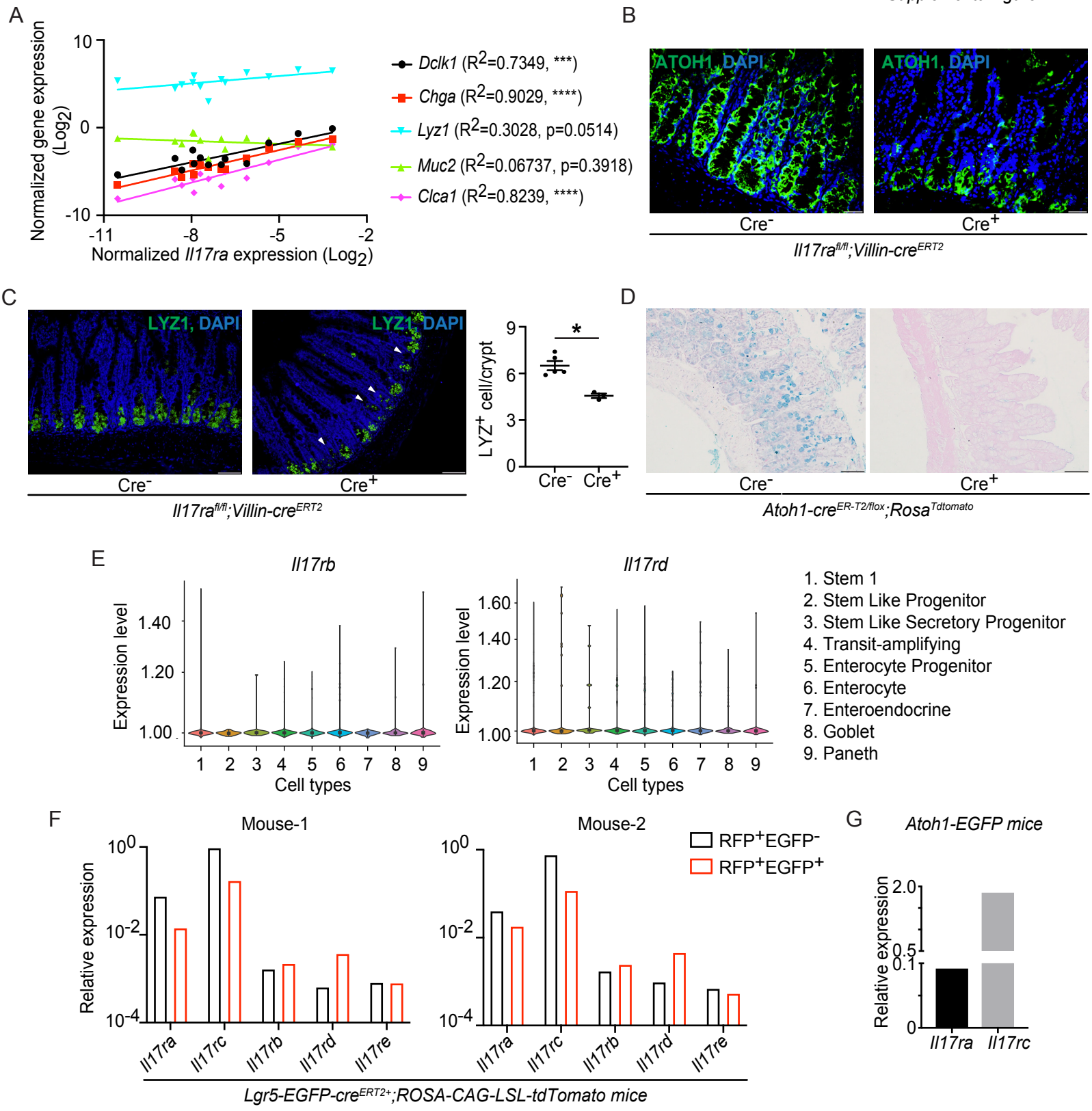
A
Normalized gene expression (Log2)
Normalized Il17ra expression (Log2)
Dclk1 (R2=0.7349, ***)
Chga (R2=0.9029, ****)
Lyz1 (R2=0.3028, p=0.0514)
Muc2 (R2=0.06737, p=0.3918)
Clca1 (R2=0.8239, ****)
B
ATOH1, DAPI
Cre-
Cre+
Il17rafl/fl;Villin-creERT2
C
LYZ1, DAPI
LYZ+ cell/crypt
Cre-
Cre+
Il17rafl/fl;Villin-creERT2
D
Cre-
Cre+
Atoh1-creER-T2/flox;RosaTdtomato
E
Il17rb
Il17rd
Expression level
Cell types
1. Stem 1
2. Stem Like Progenitor
3. Stem Like Secretory Progenitor
4. Transit-amplifying
5. Enterocyte Progenitor
6. Enterocyte
7. Enteroendocrine
8. Goblet
9. Paneth
F
Mouse-1
Mouse-2
RFP+EGFP-
RFP+EGFP+
Relative expression
Il17ra
Il17rc
Il17rb
Il17rd
Il17re
Lgr5-EGFP-creERT2+;ROSA-CAG-LSL-tdTomato mice
G
Atoh1-EGFP mice
Relative expression
Il17ra
Il17rc

Supplemental Figure 2. Characterization of IL-17 receptor expression in different cell types, related to Figures 2 and 3. A-C) *Il17ra*$^{fl/fl}$*;Villin-cre*^{ERT2} mice were injected with tamoxifen for 5 continuous days. RNA was extracted from the terminal ileum on day 11. The correlation of *Il17ra* expression with secretory markers was analyzed by RT-PCR (A). The terminal ileum was stained with anti-ATOH1 (B) or anti-LYZ1 (C, left panel). LYZ1^{+} cell/crypt is counted (C, right panel). **D)** *Atoh1-cre*$^{ER\text{-}T2/flox}$*;Rosa*^{tdtomato} mice were injected with tamoxifen for 3 continuous days. The terminal ileum was harvested at one week post the last tamoxifen injection and stained with alcian blue. **E)** Single cell RNA-seq data of C57BL/6J primary small intestinal organoids depict the expression of *Il17rb* and *Il17rd* in indicated cells of the intestinal epithelium. **F)** Cells were sorted from the small intestine of *Lgr5-EGFP-cre*$^{ERT2+}$*;ROSA-CAG-LSL-tdTomato* mice after tamoxifen injection. The expression of IL-17 receptors in the sorted cells was analyzed by RT-PCR. **G)** EGFP^{+} cells were sorted from ATOH1-EGFP mice. RT-PCR data depict the expression of *Il17ra* and *Il17rc*.

Figure S2A was generated from 2 independent experiments. Figure S2B, S2C and S2D were representative of at least 3 mice in each group. Data are presented as mean ± SEM in all graphs. Scale bars in relevant figures equal 20 μm (2B), 50 μm (2C, 2D). *$P \leq 0.05$; ***$P \leq 0.001$; ****$P \leq 0.0001$ (Simple linear regression in A and Mann-Whitney test, two-tailed in C).

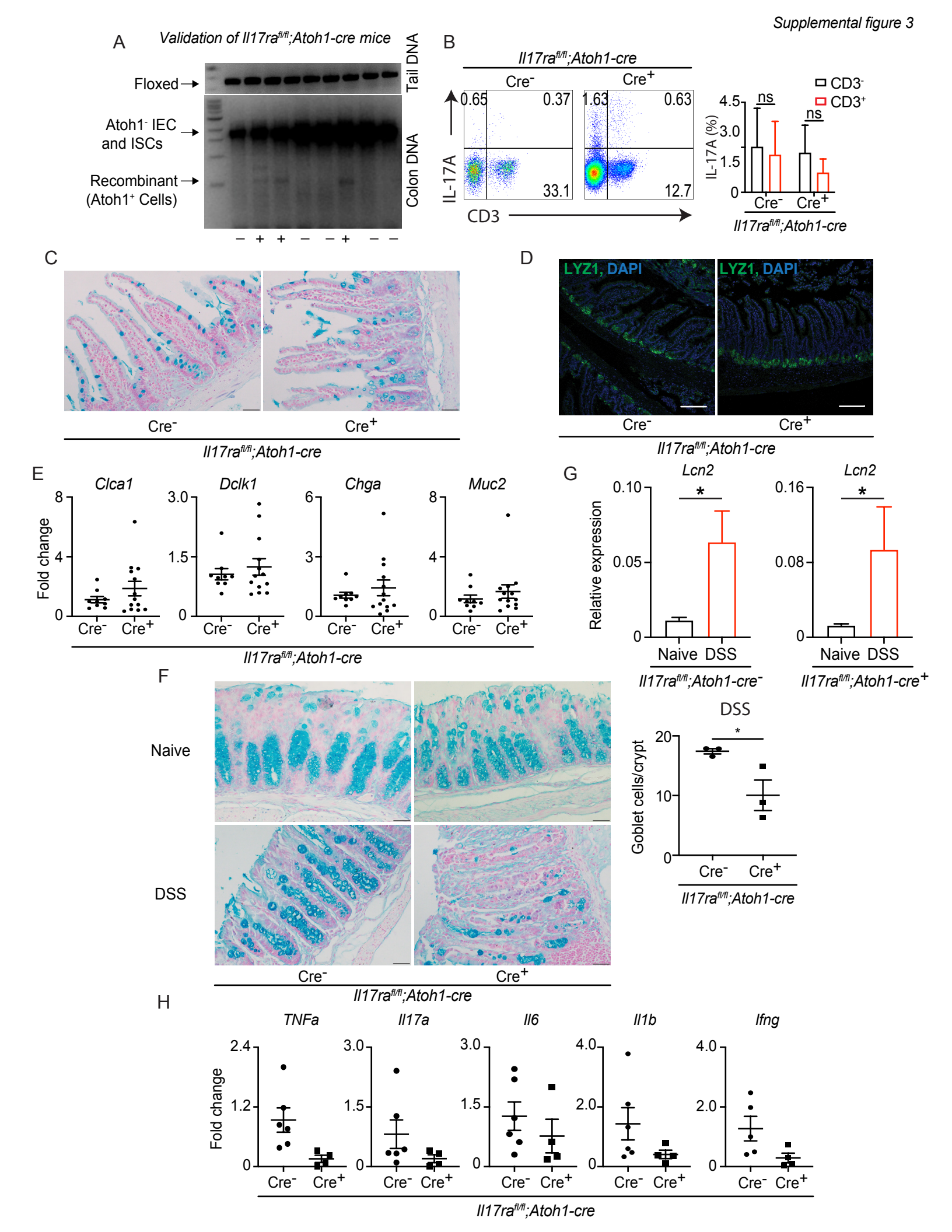
A
Validation of Il17ra^fl/fl;Atoh1-cre mice
Floxed
Atoh1- IEC and ISCs
Recombinant (Atoh1+ Cells)
Tail DNA
Colon DNA
B
Il17ra^fl/fl;Atoh1-cre
Cre-
Cre+
0.65
0.37
1.63
0.63
33.1
12.7
IL-17A
CD3
CD3-
CD3+
ns
IL-17A (%)
C
Cre-
Cre+
Il17ra^fl/fl;Atoh1-cre
D
LYZ1, DAPI
LYZ1, DAPI
E
Clca1
Dclk1
Chga
Muc2
Fold change
G
Lcn2
Relative expression
Naive
DSS
Il17ra^fl/fl;Atoh1-cre-
Il17ra^fl/fl;Atoh1-cre+
F
Naive
DSS
Goblet cells/crypt
H
TNFa
Il17a
Il6
Il1b
Ifng

Supplemental Figure 3. Characterization of *Il17ra*$^{fl/fl}$*;Atoh1-cre* mice, related to Figure 3. A-E) Agarose gel PCR shows recombination of the IL-17RA allele in the colon of naïve *Il17ra*$^{fl/fl}$*;Atoh1-cre* mice (A). Lamina propria leukocytes were isolated from the small intestine of naïve *Il17ra*$^{fl/fl}$*;Atoh1-cre* mice. IL-17A production in CD45^{+} cells was analyzed by flow cytometry (B, left panel) and the percentage was plotted (right panel). The terminal ileum was harvested at 6 weeks old and stained with alcian blue (C) and anti-LYZ1 (D). RNA was extracted from the distal colon and the expression of *Clca1*, *Dclk1*, *Chga* and *Muc2* was analyzed by RT-PCR (E). **F)** Distal colon tissues were harvested from naïve (upper row, left panel) or 2.5% DSS-treated (lower row, left panel) *Il17ra*$^{fl/fl}$*;Atoh1-cre* mice and stained with alcian blue. The number of goblet cells (alcian blue^{+}) in DSS-treated mice was counted (right panel). **G)** RT-PCR depicts the expression of *Lcn2* in the terminal ileum of *Il17ra*$^{fl/fl}$*;Atoh1-cre* mice on day 6 of 2.5% DSS treatment. **H)** The terminal ileum of *Il17ra*$^{fl/fl}$*;Atoh1-cre* mice was harvested on day 9 of 2.5% DSS followed by water treatment. The expression of *Tnfa, Il17a, Il6, Il1b and Ifng* was analyzed by RT-PCR.

Figure S3E, S3G and S3H were generated from 2-3 independent experiments. Figure S3B, S3C, S3D and S3F are representative of at least 3 mice in each group. Data are presented as mean ± SEM in all graphs. Scale bars in relevant figures equal 50 μm (3C, 3D), 20 μm (3F). *$P \leq 0.05$ (Two-way ANOVA in B, Mann-Whitney test, two-tailed in E and H, Student's t-test in F and G).

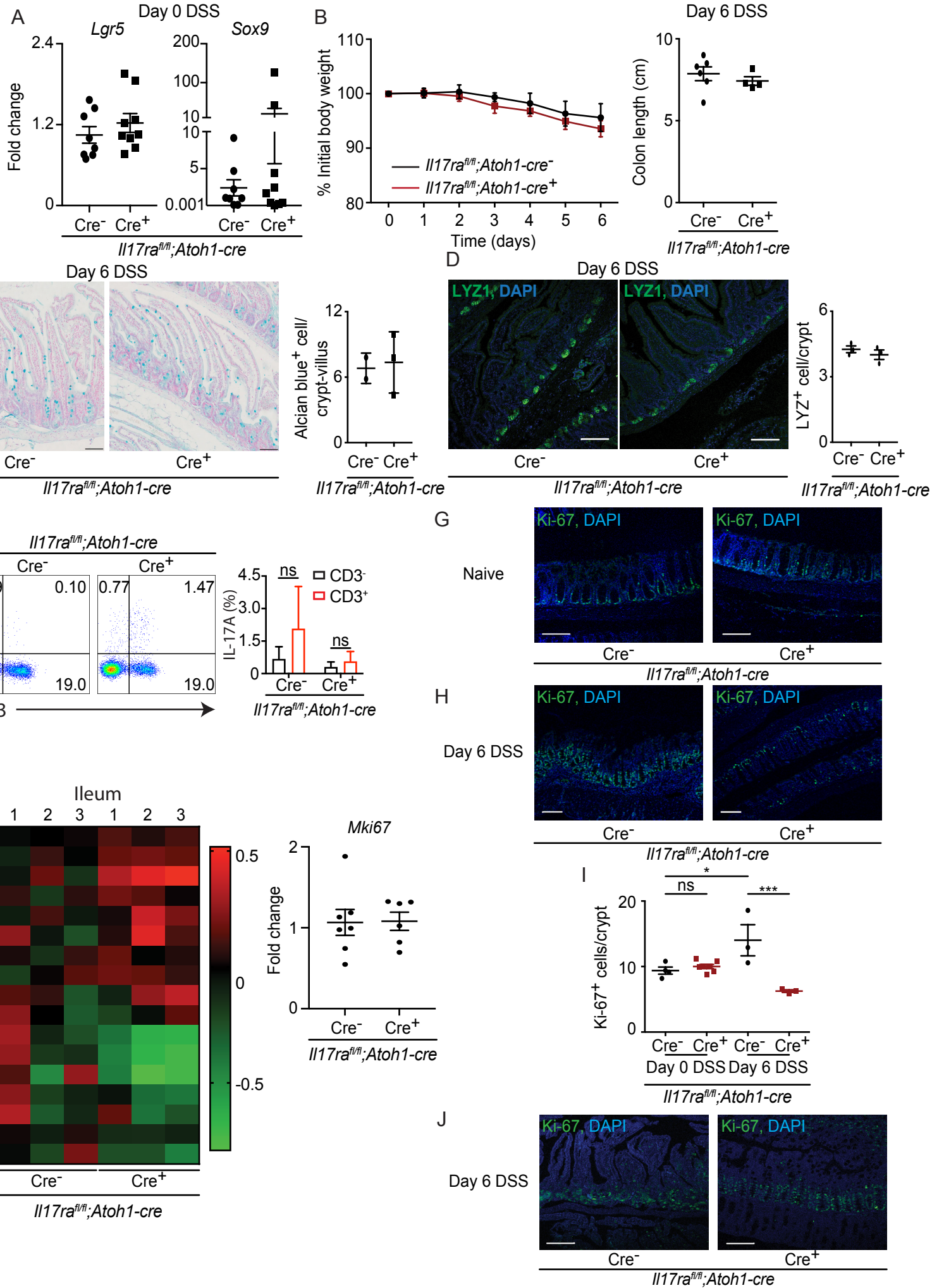
A
Day 0 DSS
Lgr5
Sox9
Fold change
Cre- Cre+
Il17ra fl/fl;Atoh1-cre
B
% Initial body weight
Time (days)
Il17ra fl/fl;Atoh1-cre-
Il17ra fl/fl;Atoh1-cre+
Day 6 DSS
Colon length (cm)
C
Day 6 DSS
Alcian blue+ cell/ crypt-villus
D
Day 6 DSS
LYZ1, DAPI
LYZ+ cell/crypt
E
Il17ra fl/fl;Atoh1-cre
IL-17A
CD3
IL-17A (%)
ns
CD3-
CD3+
F
Ileum
Lgr5
Sox9
Ascl2
Spdef
Notch1
Hes1
Atoh1
Muc2
Mki67
Cdk1
Defa26
Defa3
Defa22
Defa24
Lyz1
Atf4
Ddit3
Mki67
Fold change
G
Naive
Ki-67, DAPI
H
Day 6 DSS
I
Ki-67+ cells/crypt
Day 0 DSS Day 6 DSS
J
Day 6 DSS

Supplemental Figure 4. *Il17ra*$^{fl/fl}$*;Atoh1-cre*$^{+}$ mice did not display colonic and ileal defects after DSS treatment for 6 days, related to Figure 5. A) The terminal ileum was isolated from naïve *Il17ra*$^{fl/fl}$*;Atoh1-cre* mice and the expression of *Lgr5* and *Sox9* was analyzed by RT-PCR. **B-F)** *Il17ra*$^{fl/fl}$*;Atoh1-cre* mice were treated with 2.5% DSS for 6 days. The weight loss was recorded daily (B, left panel). The colon was harvested on day 6 and the colon length was measured (B, right panel). Terminal ileum tissues were stained with alcian blue (C, left panel) and anti-LYZ1 (D, left panel). Alcian blue^{+} cells/crypt-villus (C, right panel) and LYZ1^{+}/crypt (D, right panel) were counted. Lamina propria leukocytes were isolated from the ileum of *Il17ra*$^{fl/fl}$*;Atoh1-cre* mice on day 6 of DSS treatment. IL-17A production in CD45^{+} cells was analyzed by flow cytometry (E, left panel) and the percentage of IL-17A producing cells was graphed (E, right panel). RNA-seq depicts the gene expression in the terminal ileum harvested on day 6 of DSS treatment (F, left panel). *Mki67* expression in the terminal ileum on day 6 was further confirmed by RT-PCR (F, right panel). **G-I)** The distal colon was harvested on day 0 (G) or day 6 (H) of 2.5% DSS treatment and stained with anti-Ki-67. Ki-67^{+} cells were counted (I). **J)** The terminal ileum was harvested on day 6 of 2.5% DSS treatment and stained with anti-Ki-67.

Figure S4A and S4B were generated from two independent experiments. Except for S4C (2-3 mice), figure S4D, S4E, S4G, S4H and S4J were the representative images of at least 3 mice in each group. Data are presented as mean ± SD in S4C and mean ± SEM in other graphs. Scale bars in relevant figures equal 50 μm (4C, 4D), 100 μm (4G, 4H, 4J). *$P \leq 0.05$; ***$P \leq 0.001$ (Mann-Whitney test, two-tailed in A, B (right panel), C (right panel), D (right panel) and F, Two-way ANOVA in B (left panel) and E (right panel), One-way ANOVA in I)

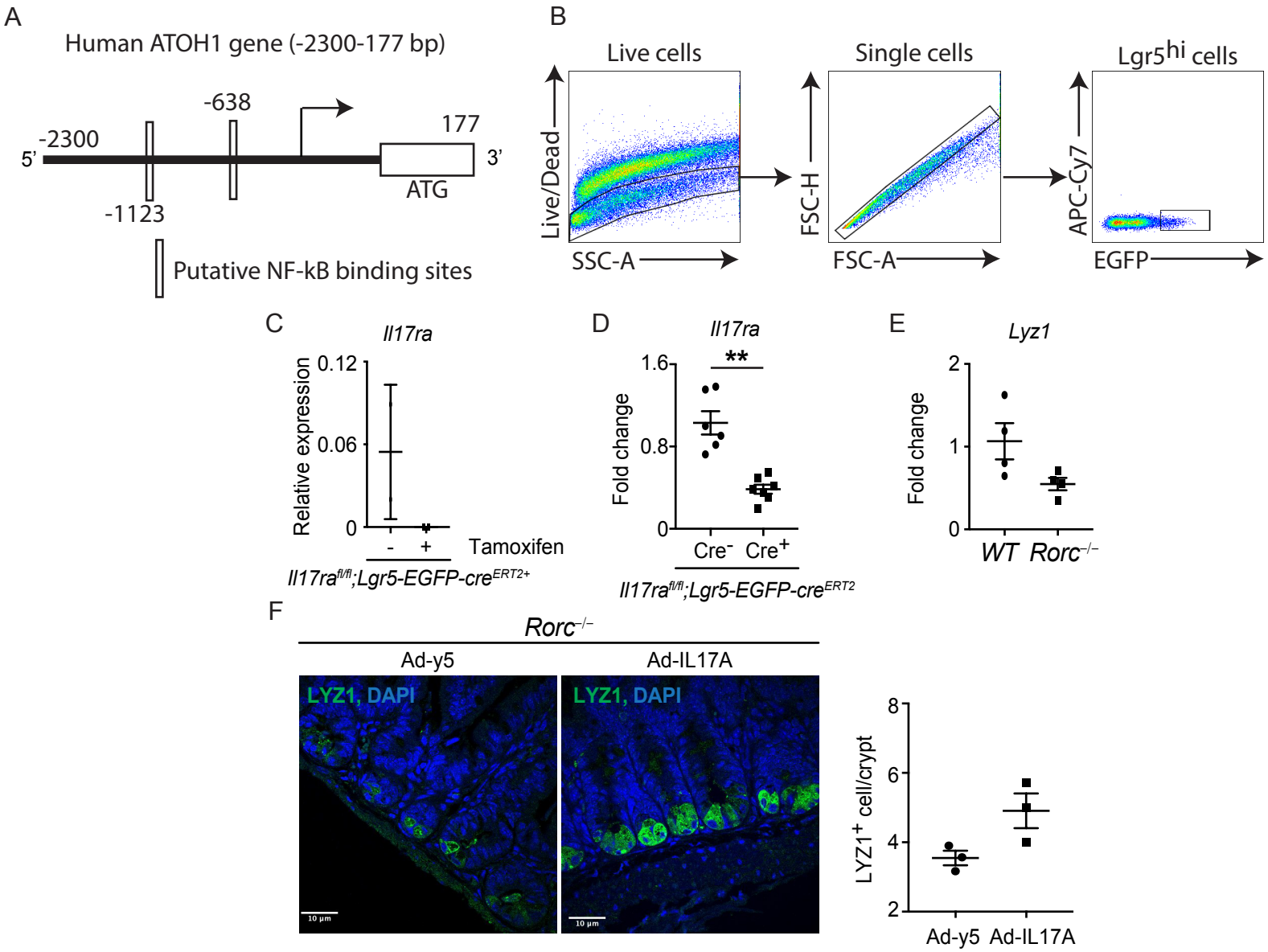

Supplemental Figure 5. IL-17A delivery leads to increased number of LYZ1⁺ cells, related to Figures 5 and 6. A) Putative NF-κB binding sites predicted in the human *ATOH1* promoter. **B)** Crypts were isolated from the ileum of *Il17ra*$^{fl/fl}$*;Lgr5-EGFP-cre*^{ERT2} mice and processed for flow cytometry. The figure shows the gating strategy for EGFP^{hi} cells (Lgr5^{+} ISCs). **C-D)** *Il17ra*$^{fl/fl}$*;Lgr5-EGFP-cre*^{ERT2} mice were injected with corn oil or tamoxifen for 5 continuous days. Crypts were isolated and EGFP^{hi} cells (Lgr5^{+} ISCs) were sorted by FACS. RT-PCR data confirmed the deletion of *Il17ra* in sorted Lgr5^{+} ISCs (C). The knockout of *Il17ra* in the terminal ileum was further demonstrated by RT-PCR (D). **E)** RT-PCR data depict *Lyz1* expression in the terminal ileum of C57BL/6J (WT) and *Rorc*$^{-/-}$ mice. **F)** *Rorc*$^{-/-}$ mice were injected with adenovirus-IL17A (Ad-IL-17A) or empty vector (Ad-Y5) and the tissues were harvested at 7 days post injection. The terminal ileum was stained with anti-LYZ1 (left panel) and the number of LYZ1+ cells/crypt was plotted (right panel).

Figure S5D was generated from two independent experiments. Figure 5E was generated from 4 mice in each group. Figure 5F is the representative image of 3 mice in each group. Data are presented as mean ± SD in S5C and mean ± SEM in other graphs. Scale bars in relevant figures equal 10 µm (5F). $^{**}P \leq 0.01$ (Mann-Whitney test, two-tailed in D-F).

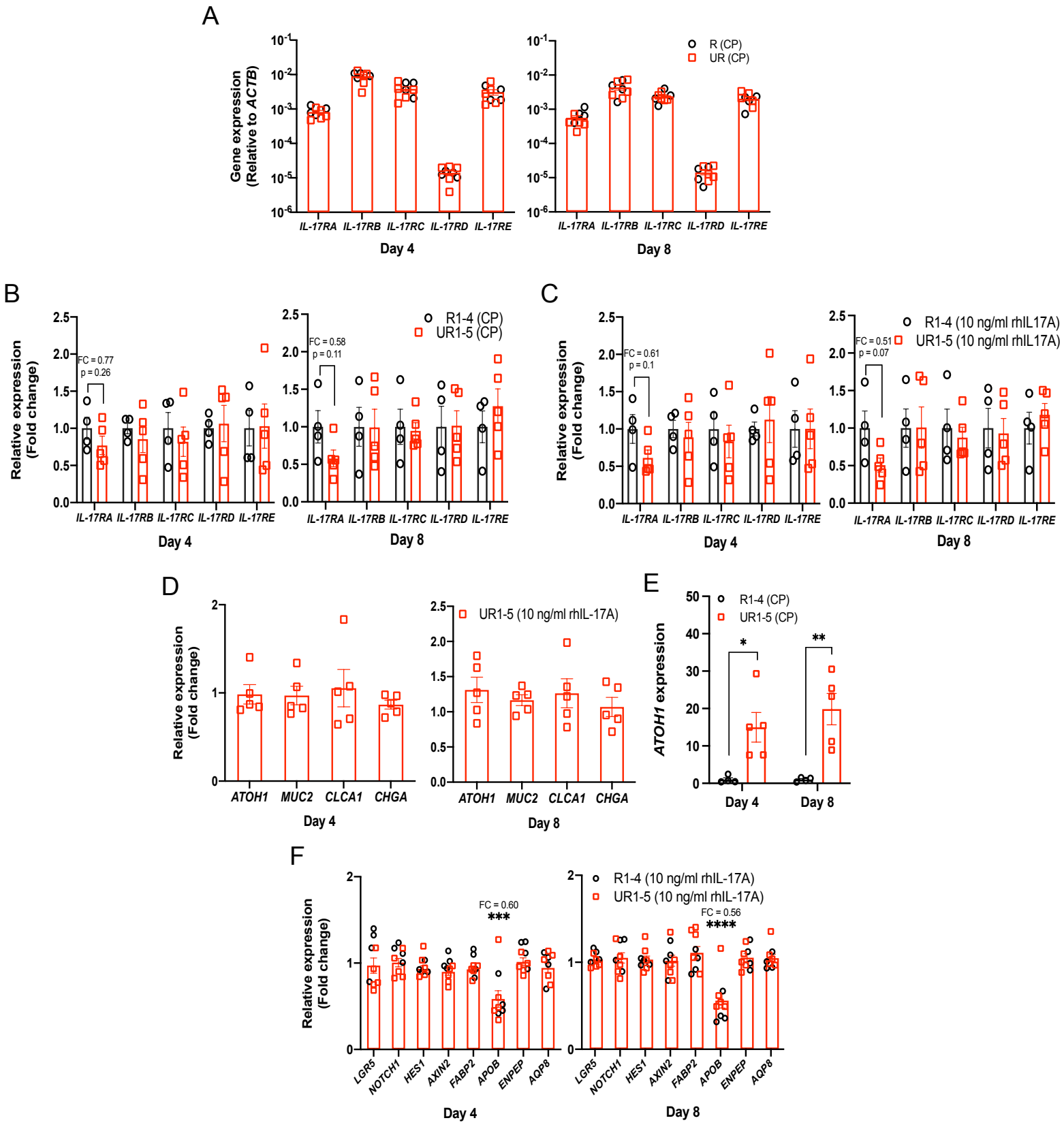
A
Gene expression (Relative to ACTB)
R (CP)
UR (CP)
IL-17RA IL-17RB IL-17RC IL-17RD IL-17RE
Day 4
Day 8
B
Relative expression (Fold change)
FC = 0.77
p = 0.26
FC = 0.58
p = 0.11
R1-4 (CP)
UR1-5 (CP)
C
FC = 0.61
p = 0.1
FC = 0.51
p = 0.07
R1-4 (10 ng/ml rhIL17A)
UR1-5 (10 ng/ml rhIL17A)
D
ATOH1 MUC2 CLCA1 CHGA
E
ATOH1 expression
F
FC = 0.60
***
FC = 0.56
****
LGR5 NOTCH1 HES1 AXIN2 FABP2 APOB ENPEP AQP8

Supplemental Figure 6. Transcript analysis of IL-17A-responsive (R) and -unresponsive (UR) lines stimulated with rhIL-17A, related to Figure 7. A) RT-PCR analysis of IL-17 receptor genes (*IL-17RA*, *IL-17RB*, *IL-17RC*, *IL-17RD*, and *IL-17RE*) among R and UR lines without rhIL-17A stimulation on days 4 (left) and 8 (right). **B and C)** Fold change of the IL-17 receptor gene expression between the R and UR lines treated with either CP (B) or rhIL-17A (C) on days 4 (left) and 8 (right). **D)** RT-PCR data depicting *ATOH1*, *MUC2*, *CLCA1*, and *CHGA* expression among the rhIL-17A-stimulated UR lines on days 4 (left) and 8 (right). **E)** RT-PCR analysis of *ATOH1* expression in the R or UR lines on days 4 and 8. **F)** Fold change of *LGR5*, *NOTCH1*, *HES1*, *AXIN2*, *FABP2, APOB*, *ENPEP*, and *AQP8* expression among the rhIL-17A-stimulated R and UR lines on days 4 (left) and 8 (right).

Data points in A-F are mean of three technical replicates of individual lines. Bars represent mean ± SEM, and at least three independent experiments were performed. CP, carrier protein; FC, fold change. *$P \leq 0.05$; **$P \leq 0.01$; ***$P \leq 0.001$; ****$P \leq 0.0001$ (unpaired t test, two-tailed in A-F).

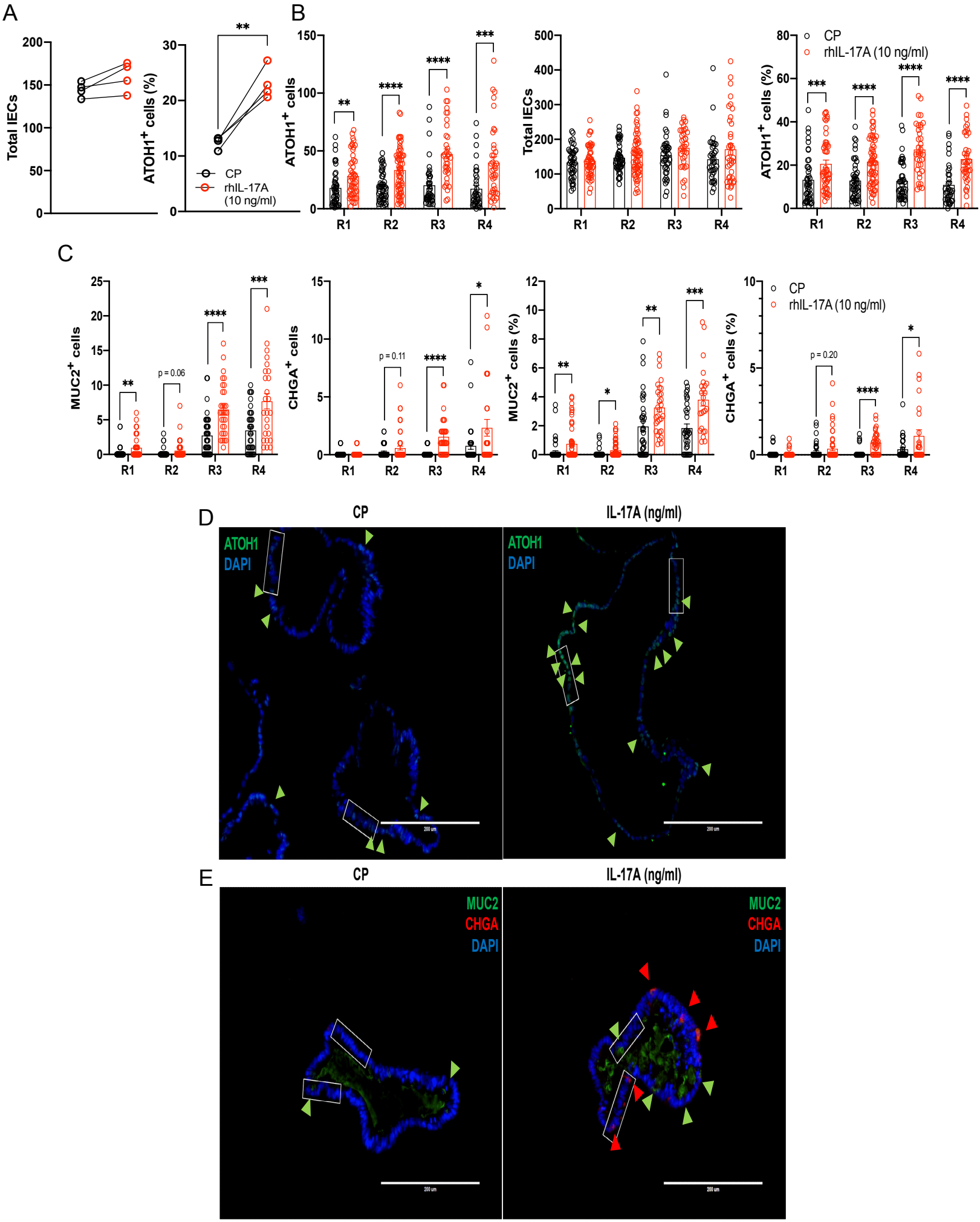
A
Total IECs
ATOH1+ cells (%)
CP
rhIL-17A (10 ng/ml)
B
ATOH1+ cells
Total IECs
ATOH1+ cells (%)
CP
rhIL-17A (10 ng/ml)
R1
R2
R3
R4
C
MUC2+ cells
CHGA+ cells
MUC2+ cells (%)
CHGA+ cells (%)
p = 0.06
p = 0.11
p = 0.20
D
CP
IL-17A (ng/ml)
ATOH1
DAPI
E
MUC2
CHGA
DAPI

Supplemental Figure 7. Immunohistochemistry analysis of IL-17A-responsive (R) and -unresponsive (UR) lines stimulated with rhIL-17A, related to Figure 7. A) Total number of IECs (left) and frequency of ATOH1$^+$ cells normalized to total IECs (right) among the rhIL-17A-stimulated R lines on day 8. **B)** Total number of ATOH1$^+$ cells (left), total number of IECs (middle), and frequency of ATOH1$^+$ cells per total IECs (right) in each visual field from R lines with or without rhIL-17A stimulation on day 8. **C)** Total number of MUC2$^+$ or CHGA$^+$ cells (left) and frequency of MUC2$^+$ or CHGA$^+$ cells normalized to total IECs (right) in each visual field from R lines with or without rhIL-17A stimulation on day 8. **D and E)** Enlarged ATOH1 staining images (D) and MUC2 and CHGA co-staining images (E) in the rhIL-17A-stimulated R lines on day 8. Bars: 200 μm. Data points in B and C represent visual field. Bars represent mean ± SEM, and at least three independent experiments were performed. CP, carrier protein. *$P \leq 0.05$; **$P \leq 0.01$; ***$P \leq 0.001$; ****$P \leq 0.0001$ (paired t test, two-tailed in A, unpaired t test, two-tailed in B and C).

Name	Tissue	Sex	Age	Disease type	Inflammation	Organoid
R1	Duodenum	M	37	CD	Non-inflamed	Cystic
R2	Duodenum	F	67	CD	Non-inflamed	Cystic
R3	Terminal ileum	F	25	Non-IBD	Non-inflamed	Cystic
R4	Terminal ileum	M	34	Non-IBD	Non-inflamed	Cystic
UR1	Terminal ileum	M	37	CD	Non-inflamed	Budding
UR2	Terminal Ileum	M	47	CD	Non-inflamed	Budding
UR3	Terminal ileum	M	23	CD	Non-inflamed	Budding
UR4	Terminal ileum	F	47	Non-IBD	Non-inflamed	Budding
UR5	Terminal ileum	M	29	Non-IBD	Non-inflamed	Budding

Supplemental Table 1. Subject information for human endoscopic specimens. Related to Figure 7.

M; Male, F; Female, CD; Crohn's disease.

Target	Organism	Forward 5'-3'	Reverse 5'-3'
Il6	*Mus musculus*	TCCAATGCTCTCCTAACAGATAAG	CAAGATGAATTGGATGGTCTTG
Sox9	*Mus musculus*	AGTACCCGCATCTGCACAAC	ACGAAGGGTCTCTTCTCGCT
Pigr	*Mus musculus*	ATGAGGCTCTACTTGTTCACGC	CGCCTTCTATACTACTCACCTCC
Lgr5	*Mus musculus*	CTACTCGAAGACTTACCCAGT	GCATTGGGGTGAATGATAGCA
Hes1	*Mus musculus*	TGCCTTTCTCATCCCCAACG	AGGTGACACTGCGTTAGGAC
Lcn2	*Mus musculus*	GGGAAATATGCACAGGTATCCTC	CATGGCGAACTGGTTGTAGTC
Apob	*Mus musculus*	AAGCACCTCCGAAAGTACGTG	CTCCAGCTCTACCTTACAGTTGA
Enpep	*Mus musculus*	ATAGTGGGACTTTCTGTGGGT	GGTCGTAGTGAACTGGATTGATG
Aqp8	*Mus musculus*	TGTGTAGTATGGACCTACCTGAG	ACCGATAGACATCCGATGAAGAT
Il17rb	*Mus musculus*	GGCTGCCTAAACCACGTAATG	CCCGTTGAATGAGAATCGTGT
Il17rd	*Mus musculus*	AACAGCGGACTGCACAACAT	GCAAGCGTACTGGCTGATG
Il17re	*Mus musculus*	CAGTCCCAGTGACGCTAGAC	ACCCACTAGAGCGGTGAGAG
Lrig1	*Mus musculus*	TTGAGGACTTGACGAATCTGC	CTTGTTGTGCTGCAAAAAGAGAG
Dll1	*Mus musculus*	GCAGGACCTTCTTTCGCGTAT	AAGGGGAATCGGATGGGGTT
Ifng	*Mus musculus*	ATGAACGCTACACACTGCATC	CCATCCTTTTGCCAGTTCCTC
Il1b	*Mus musculus*	GCAACTGTTCCTGAACTCAACT	ATCTTTTGGGGTCCGTCAACT
IL17RA	*Homo sapiens*	TTCTGTCCAAACTGAGGCATCA	AGGGTCAACCACAAAGTGGC
IL17RB	*Homo sapiens*	GCCCTTCCATGTCTGTGAA	CAGGGGAGTGGTTGTGAAGT
IL17RC	*Homo sapiens*	GCCCCATGGACAAATACATC	ATCGGCTGAGTAGAGGAGCA
IL17RD	*Homo sapiens*	CTGTCTCTGCCACTGATGGA	CCAAGATCTGCTTTGCATGA
IL17RE	*Homo sapiens*	CTGCTGTCAGGTGGCTCA	GGAAGACTTTTTGGATTTCTGC
ATOH1	*Homo sapiens*	GTCCGAGCTGCTACAAACG	GTGGTGGTGGTCGCTTTT
MUC2	*Homo sapiens*	GCTGCTATGTCGAGGACACC	GGGAGGAGTTGGTACACACG
CLCA1	*Homo sapiens*	GCTGATGTTCTGGTTGCTGA	CGTCAAATACTCCCCATCGT
CHGA	*Homo sapiens*	TGTAGTGCTGAACCCCCACC	CTCTCGCCTTTCCGGATCT
LGR5	*Homo sapiens*	CAGCGTCCTCACCTCCTACC	TGGGAATGTATGTCAGAGCG
NOTCH1	*Homo sapiens*	CGCACAAGGTGTCTTCCAG	AGGATCAGTGGCGTCGTG
HES1	*Homo sapiens*	AGTGAAGCACCTCCGGAAC	CGTTCATGCACTCGCTGA
AXIN2	*Homo sapiens*	AGTGTGAGGTCCACGGAAAC	CTGGTGCAAAGACATAGCCA
FABP2	*Homo sapiens*	AACTGAACTCAGGGGGACCT	CCTTTTGGCTTCTACTCCTTCA
APOB	*Homo sapiens*	GGAGCTGCTGGACATTGCTA	ATGGCAGCTTTCTGGATCAT
ENPEP	*Homo sapiens*	TGACACCGTTCACGTTAAGCA	GGAAGAGGCAAGTAGGCTACCA
AQP8	*Homo sapiens*	GCGAGTGTCCTGGTACGAAC	CAGGCACCCGATGAAGATGAA
ACTB	*Homo sapiens*	CCCAGCCATGTACGTTGCTA	TCACCGGAGTCCATCACGAT

Supplemental Table 2. Primer sequences for qPCR. Related to STAR Methods.